

Synthesis, Characterization, and Structure Determination of a New Heterometallic Oxoalkoxide: $\text{Er}_2\text{Ti}_4\text{O}_2(\text{OC}_2\text{H}_5)_{18}(\text{HOC}_2\text{H}_5)_2$

G. Westin,* R. Norrestam,† M. Nygren,* and M. Wijk*

*Department of Inorganic Chemistry and †Department of Structural Chemistry, and Arrhenius Laboratory, Stockholm University, S-10691 Stockholm, Sweden

Received July 2, 1996; in revised form June 5, 1997; accepted September 9, 1997

Different synthesis routes have been studied for the preparation of a new oxoalkoxide, $\text{Er}_2\text{Ti}_4\text{O}_2(\text{OEt})_{18}(\text{HOEt})_2$ ($\text{Et} = \text{C}_2\text{H}_5$). The compound was best prepared by reacting KOEt and $\text{Ti}(\text{OEt})_4$ first with water and then with ErCl_3 . The structure was determined by single-crystal X-ray diffraction, showing the unit cell to have the monoclinic space group symmetry, $P2_1/n$, and the lattice constants $a = 15.180(2) \text{ \AA}$, $b = 12.693(2) \text{ \AA}$, $c = 16.602(3) \text{ \AA}$ and $\beta = 98.91(1)^\circ$ and to contain two formula units. The final R value was 0.053 ($wR = 0.077$). The molecule contains three of the most commonly found structure fragments of alkoxides, namely the C_{2h} fragment of $\text{Ti}_4(\text{OEt})_{16}(\text{Er}_2\text{Ti}_2\text{O}_6)$, the $M_4(\mu_4\text{-O})$ fragment ($\text{Er}_2\text{Ti}_2\text{O}$), and the face-sharing MO_6 octahedra, with $M = \text{Ti}^{4+}$. IR studies revealed that the molecular structure of the alkoxide was retained to a large extent when the alkoxide was dissolved in 4:1 ethanol:toluene and hexane solvents. © 1998 Academic Press

1. INTRODUCTION

In recent years, the interest in metal alkoxides and their use in designing new materials has grown enormously (1, 2). The range of applications is wide, mainly concerning electrical and optical materials. For optical applications, such as laser amplifiers and up-conversion devices in the forms of waveguides and bulk glasses containing Ln^{3+} ions, mainly Er^{3+} and Nd^{3+} are of special interest. The formation of Ln -rich oxide clusters, which often occurs with solid-state synthesis and sol-gel processing of solutions containing Er^{3+} salts, decreases the optical activity. One approach to avoid such cluster formation, which is investigated by our group, is to encapsulate the Ln atom by optically silent metal atoms in the precursor alkoxide molecule. Optically silent metal atoms can be, e.g., B, Al, Ti, Zr, or Nb. In an earlier publication we described a heterometallic alkoxide that contains an isolated Er atom surrounded by optically silent metal atoms (Al) bonded to Er via isopropoxo bridges (3).

In this paper, we present a new oxoalkoxide, $\text{Er}_2\text{Ti}_4\text{O}_2(\text{OEt})_{18}(\text{HOEt})_2$. The structure determination of this

compound showed that each molecule contains two Er atoms directly connected, via bridging oxo-oxygen atoms, which means that it is unsuitable for the previously mentioned investigation. Nevertheless, the structure of this molecule is interesting, as it contains three of the most common structure fragments, familiar from other alkoxides.

The structures of several metal alkoxides containing titanium have been determined (4–15). In many cases, pairwise face-sharing Ti octahedra are found in these alkoxides. This fragment is also observed in other M^{4+} -containing alkoxides. e.g., Zr (16), Ce (17), and U (18).

Since we could not isolate any heterobimetallic alkoxides when using rigorously dry and oxygen-free conditions, we have made a study of different synthesis routes to obtaining the isolable oxoalkoxide $\text{Er}_2\text{Ti}_4\text{O}_2(\text{OEt})_{18}(\text{HOEt})_2$.

2. EXPERIMENTAL

2.1. Synthesis

All preparations and the mounting of the crystals for the X-ray data collection were performed in a glovebox containing a dry, oxygen-free nitrogen or argon atmosphere. The ethanol used was dried by distillation over CaH_2 and the toluene was dried with thin slices of sodium. Commercial anhydrous ErCl_3 (Strem Chemicals), erbium metal (Aldrich, 99.9%), potassium (Aldrich), and $\text{Ti}(\text{OEt})_4$ (Fluka, 97%) were used.

Since only an oxoalkoxide could be isolated in crystalline form, we made a study of different pathways to obtaining this oxo compound:

Route 1. Typically, 12.6 mmol (0.493 g) of potassium was dissolved in 70 ml of 4:1 (vol:vol) toluene:ethanol solvent, and then 8.41 mmol (1.92 g) of titanium tetraethoxide was added. After 2 h, 4.20 ml of 1 M H_2O in 4:1 toluene:ethanol was added dropwise, and 2 h later, 4.203 mmol (1.150 g) of ErCl_3 was added. The reaction was allowed to proceed for 48 h, whereupon the mixture was centrifuged to separate the KCl precipitate. An electronic spectrum of the solution, in the range 515–540 nm, is shown in Fig. 1.

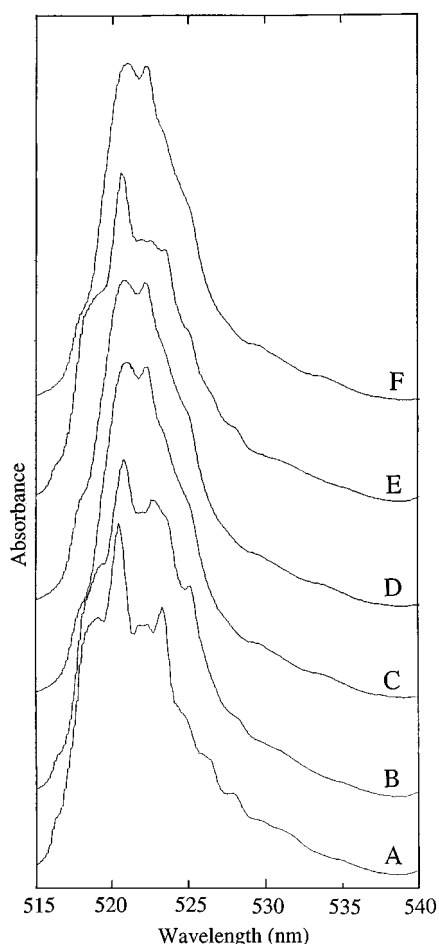


FIG. 1. Spectra showing the ${}^2H_{11/2} \leftarrow {}^4I_{15/2}$ absorption band of the Er^{3+} ion in solutions from redissolved $\text{Er}_2\text{Ti}_4\text{O}_2(\text{OEt})_{18}(\text{HOEt})_2$ in 4:1 toluene:ethanol (A); route 1 (B); route 2A, before the addition of oxygen (C); route 2A, after the oxygen addition (D); route 2B (E); route 3 (F).

Evaporation of the solution yielded a crystal mass, which after washing with ethanol was identified as being $\text{Er}_2\text{Ti}_4\text{O}_2(\text{OEt})_{18}(\text{HOEt})_2$ (yields 70–80%). An electronic spectrum of the redissolved crystals is shown in Fig. 1. FT-IR spectra of the compound, as solid and solution, are shown in Fig. 3. Recrystallization can be achieved by dissolution in toluene followed by addition of ethanol.

Route 2A. Metathesis, carried out in the same way as in route 1, but without addition of water, yielded a pink solution from which almost no crystals were obtained on evaporation. Instead, a viscous solution was formed which did not crystallize for months. After ethanol addition, crystallization occurred very slowly (over many weeks). An electronic spectrum of the solution before evaporation is shown in Fig. 1. Addition of dry oxygen gas for 48 h, to the solution obtained before evaporation changed the

electronic spectrum of the solution only marginally (see Fig. 1). The yields of $\text{Er}_2\text{Ti}_4\text{O}_2(\text{OEt})_{18}(\text{HOEt})_2$ on evaporation were only a few percent.

Route 2B. Metathesis was carried out in the same way as in route 2A, but with addition of 1 equivalent of water per Er, as 1 M H_2O in 4:1 toluene:ethanol, instead of oxygen. An electronic spectrum of the solution before evaporation is shown in Fig. 1. Evaporation gave crystals of $\text{Er}_2\text{Ti}_4\text{O}_2(\text{OEt})_{18}(\text{HOEt})_2$ in yields of ca. 70%.

Route 3. Metathesis, in the same way as in route 2A, before the oxygen addition, but at 65°C for 120 h, yielded a solution whose electronic spectrum is shown in Fig. 1, and evaporation of it afforded less than a few percent of crystals.

Route 4. Er metal (2.20 mmol (0.368 g)) 6 ml of 4:1 toluene:ethanol solvent, 0.3 ml of ethanol, 4.4 mmol (1.0 g) of titanium tetraethoxide, and ca. 1 mg of HgCl_2 were mixed and reacted at 60°C for 48 h. The solution part was purple after 24 h and pale yellow after 48 h. The electronic spectra of the solutions obtained after 24 and 48 h, respectively, are shown in Fig. 2. Evaporation of the purple solution obtained after 24 h did not yield any crystals of $\text{Er}_2\text{Ti}_4\text{O}_2(\text{OEt})_{18}(\text{HOEt})_2$, but a mixture of a dark powder and a liquid. Evaporation of the yellow solution, on the other hand, produced crystals of $\text{Er}_2\text{Ti}_4\text{O}_2(\text{OEt})_{18}(\text{HOEt})_2$ in yields of about 20–50%.

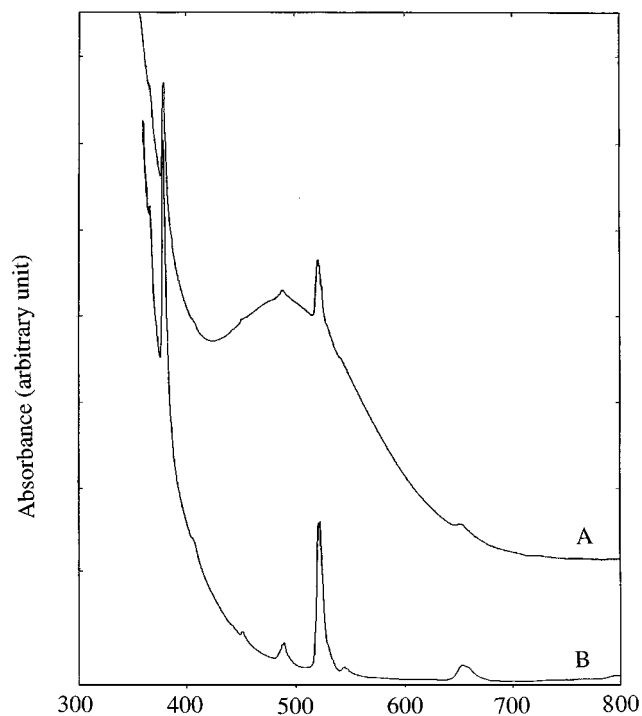


FIG. 2. Spectra of solutions of route 4 obtained after 24 (A) and 48 h (B).

2.2. Characterization

The overall metal composition was determined on isolated crystals, crystal masses, or solutions, which had been hydrolyzed and dried prior to analysis, with a scanning electron microscope (SEM, JEOL 820) equipped for energy-dispersive analysis of X-ray spectra (LINK AN 10000). The EDS determinations are judged as being within 2 mol% units for Ti and Er, from comparisons with standards. FT-IR spectra were recorded with a Bruker IFS 55 spectrometer equipped with a KBr beamsplitter and a DTGS detector. The solid samples were investigated as KBr tablets and the neat, viscous alkoxides were enclosed between KBr plates. The identity and homogeneity of the synthesis products were checked by IR studies on a large number of samples taken from different parts of the products. The dissolved samples were contained in 0.1-mm KBr cells. The electronic spectra were obtained with a Philips PU 8740 dispersive spectrometer in the range 190–900 nm using sealed quartz cells. The behavior on heating was studied with a differential scanning calorimeter (DSC, Perkin-Elmer DSC-2) using sealed steel compartments in the temperature range 25–225°C as well as in sealed glass capillaries in a solid-block melting-point apparatus in the temperature range 25–320°C.

2.3. Structure Determination

A few selected crystals, prepared as described in section 2.1, were mounted in glass capillaries ($\Phi = 1.0$ mm) that were melt-sealed in the glovebox. Preliminary single-crystal X-ray diffractometer investigations of the finally selected crystal, using $\text{MoK}\alpha$ radiation, indicated a monoclinic space group symmetry, $P2_1/n$. The crystal had a minor twin component, but as the final results show, the effects from twinning were negligible. The unit cell parameters were determined and refined, from the θ values of 12 accurately centered reflections, as $a = 15.180(2)$ Å, $b = 12.693(2)$ Å, $c = 16.602(3)$ Å, and $\beta = 98.91(1)^\circ$. Single-crystal X-ray diffraction data were collected at room temperature (22°C) on a Siemens P4/RA diffractometer. No correction for absorption effects was made due to difficulties in determining the crystal faces.

Preliminary Er positions were obtained by conventional heavy-atom techniques. The remaining non-hydrogen atomic positions were found from subsequent calculations of difference electron density ($\Delta\rho$) maps. The hydrogen atoms were positioned by assuming ideal geometry of the ethyl groups, and their positions were refined by constraining the carbon-to-hydrogen distance to be 1.0 Å. Due to the large thermal vibrations and the limited accuracy of the ethoxo group geometries, the C_α to C_β distances were softly constrained. In the final refinement, all the metal and the oxygen atoms were allowed to vibrate anisotropically,

TABLE 1
Crystallographic Data for the Structural Investigation
of $\text{Er}_2\text{Ti}_4\text{O}_2(\text{OEt})_{18}(\text{HOEt})_2$

Formula	$\text{Er}_2\text{Ti}_4\text{O}_2(\text{OEt})_{18}(\text{HOEt})_2$
Formula weight	1461.54 g/mol
Space group	$P2_1/n$
Unit cell dimensions	$a = 15.180(2)$ Å $b = 12.693(2)$ Å $c = 16.602(3)$ Å $\beta = 98.91(1)^\circ$
Volume	$3160(2)$ Å ³
Z	2
Calculated density	1.533 g/cm ³
Radiation	$\text{MoK}\alpha$
Wavelength	0.71073 Å
μ	3.17 mm ⁻¹
Temperature	22°C (295 K)
Crystal shape	Irregular
Crystal size	$0.26 \times 0.16 \times 0.22$ mm ³
Diffractometer	Siemens P4/RA
Determination of unit cell	
Number of reflections used	12
θ range of reflections used	11.2–24.1
Intensity data collection	ω - 2θ scan technique
Max of $\sin \theta/\lambda$	0.98 Å ⁻¹
Range of $h, k, \text{ and } l$	–1 to 21, –1 to 17, and –23 to 23
Standard reflections	3
Number of measured reflections	12086
Number of unique reflections	9204
Number of observed reflections	2586
Criterion for observed reflections	$I > 5\sigma(I)$
R_{int}	0.058
Structure determination technique	
Determination of H atoms	
Structure refinement	Least squares structure refinement
Minimization of	$\sum \omega (\Delta F)^2$
Anisotropic model for	Er, Ti, and O
Isotropic model for	C and H
Parameters fixed for	C and H
Number of parameters	208
Weighting scheme	$1/(\sigma^2(F) + 0.002 \times F^2)$
Final R	0.053
Final wR	0.077
Max final Δ/σ	0.055
Max and min $\Delta\rho$	1.24 and -1.66 e ⁻ Å ⁻³

while the carbon and the hydrogen atoms were held isotropic.

Details of the experimental conditions and the final structural refinements are given in Table 1. Least-squares refinements of the structural model yielded an R value of 0.053 ($wR = 0.077$). The final atomic coordinates with thermal parameters, bond distances, and selected bond angles are listed in Tables 2–5. The atomic scattering factors used were those for neutral atoms given in “International Tables for X-Ray Crystallography” (19). The SHELXTL program package (20) was used for the crystallographic calculations.

3. RESULTS AND DISCUSSION

3.1. Synthesis of $\text{Er}_2\text{Ti}_4\text{O}_2(\text{OEt})_{18}(\text{HOEt})_2$

Straightforward synthesis from ErCl_3 , KOEt, and $\text{Ti}(\text{OEt})_4$ yielded soluble Er and Ti alkoxide(s) that could

TABLE 2
Fractional Atomic Coordinates ($\times 10_4$) and Isotropic Thermal Parameters ($\times 10_3$) with e.s.d.'s for the Metal, Oxygen, and Carbon Atoms of $\text{Er}_2\text{Ti}_4\text{O}_2(\text{OEt})_{18}(\text{HOEt})_2$

Atom	x	y	z	U_{eq} (\AA^2)
Er	325(1)	1262(1)	598(1)	47(1)
Ti1	-765(3)	-268(3)	1697(2)	53(2)
Ti2	-1733(3)	470(3)	153(2)	54(2)
O1	-1085(8)	1271(8)	1213(6)	63(4)
O2	-587(7)	-256(7)	566(6)	46(4)
O3	421(8)	270(8)	1888(6)	60(4)
O4	1820(7)	544(9)	702(7)	57(4)
O5	-2045(7)	-408(9)	1082(7)	61(5)
O6	-1055(7)	1511(7)	-319(6)	53(4)
O7	-653(9)	-1731(9)	1839(7)	69(5)
O8	679(10)	2527(9)	1349(7)	84(6)
O9	749(9)	2497(8)	-352(7)	68(5)
O10	-2785(10)	1045(10)	-73(9)	85(6)
O11	-1069(9)	35(10)	2673(7)	73(5)
C1A	-1470(14)	2090(14)	1606(11)	77(6)
C1B	-1625(15)	3073(16)	1156(13)	97(7)
C3A	875(13)	629(15)	2666(11)	77(6)
C3B	1297(16)	-217(17)	3182(14)	111(8)
C4A	2549(14)	841(16)	1335(13)	84(6)
C4B	3083(19)	1618(21)	1121(18)	140(10)
C5A	-2884(24)	-384(26)	1352(21)	168(13)
C5B	-3225(27)	-1371(27)	1357(25)	213(17)
C6A	-1351(13)	1929(13)	-1141(10)	67(5)
C6B	-1605(15)	3011(15)	-1146(14)	100(7)
C7A	-633(25)	-2330(24)	2543(21)	172(13)
C7B	-623(26)	-3351(25)	2625(23)	193(15)
C8A	996(22)	3198(23)	1905(19)	152(11)
C8B	694(24)	4160(26)	1942(21)	196(15)
C9A	805(24)	3679(24)	311(23)	176(14)
C9B	1602(25)	4114(32)	-318(23)	210(17)
C10A	-3749(51)	1183(50)	-525(40)	397(42)
C10B	-4007(36)	1996(42)	-125(33)	321(27)
C11A	-1452(16)	444(20)	3323(13)	104(7)
C11B	-985(20)	154(25)	4058(16)	169(13)

not be crystallized by evaporation or addition of ethanol solvent. An electronic spectrum of the compound(s) in solution showed a fine structure of the peak, assigned as due to the ${}^2H_{11/2} \leftarrow {}^4I_{15/2}$ transition of the Er^{3+} ion (21), that was different from that of the title compound (see Fig. 1). Similar differences were also observed for the peaks assigned as due to the ${}^4G_{11/2} \leftarrow {}^4I_{15/2}$ and ${}^4F_{9/2} \leftarrow {}^4I_{15/2}$ transitions. SEM-EDS analysis of a hydrolyzed sample of the solution showed it to contain no K or Cl and that the Er to Ti ratio was close to 1:2. Evaporation of all solvent by vacuum yielded a pink viscous liquid. Its IR spectrum differed from those of $\text{Er}_2\text{Ti}_4\text{O}_2(\text{OEt})_{18}(\text{HOEt})_2$ and $\text{Ti}(\text{OEt})_4$. The liquid did not give an OH stretch band as is the case for $\text{Er}_2\text{Ti}_4\text{O}_2(\text{OEt})_{18}(\text{HOEt})_2$. We believe that the compound(s) formed without addition of water or oxygen contain no oxo oxygens. The fact that it has not been possible to obtain crystals

TABLE 3
Selected Intramolecular Distances with E.s.d.'s for $\text{Er}_2\text{Ti}_4\text{O}_2(\text{OEt})_{18}(\text{HOEt})_2$

Atoms	Distance (\AA)
Er-O1	2.51(2)
Er-O2	2.37(1)
Er-O3	2.47(1)
Er-O4	2.43(1)
Er-O6	2.41(1)
Er-O8	2.05(1)
Er-O9	2.38(1)
Er-O2A	2.40(1)
Ti1-O1	2.14(1)
Ti1-O2	1.94(1)
Ti1-O3	1.91(2)
Ti1-O5	2.06(1)
Ti1-O7	1.88(2)
Ti1-O11	1.79(2)
Ti2-O1	2.14(1)
Ti2-O2	1.99(1)
Ti2-O5	2.02(2)
Ti2-O6	1.92(1)
Ti2-O10	1.74(2)
Ti2-O4A	1.91(1)

from the solution might be due to a weak bond between the Er and Ti alkoxides or due to a formation of several different alkoxides.

In many cases, decomposition of alkoxides to form oxo alkoxides can occur on heating, and we have therefore heat-treated the synthesis mixture at 65°C for 120 h (route 3). Only very minor amounts of $\text{Er}_2\text{Ti}_4\text{O}_2(\text{OEt})_{18}(\text{HOEt})_2$ were obtained when the solution was evaporated, which might be due to a very small amount of water, unintentionally added with the reactants. The fine structure of the ${}^2H_{11/2} \leftarrow {}^4I_{15/2}$ peak was almost identical with that obtained without heating, as can be seen in Fig. 1. This

TABLE 4
Selected Intramolecular Bond Angles with E.s.d.'s, for Metal-Oxygen-Metal Bonds in $\text{Er}_2\text{Ti}_4\text{O}_2(\text{OEt})_{18}(\text{HOEt})_2$

Bonds	Angle (deg)	Bonds	Angle (deg)
Er-O2-ErA	106.3(4)	Er-O1-Ti1	89.5(4)
		Er-O1-Ti2	88.6(4)
		Er-O2-Ti1	98.9(4)
		Er-O2-Ti2	96.2(3)
Ti1-O1-Ti2	85.6(4)	ErA-O2-Ti1	147.3(4)
Ti1-O2-Ti2	95.3(4)	ErA-O2-Ti2	102.3(4)
Ti1-O5-Ti2	90.9(5)	Er-O3-Ti1	96.4(4)
		Er-O4-Ti2A	104.1(4)
		Er-O6-Ti2	96.9(4)

TABLE 5
Selected Intramolecular Bond Angles with E.s.d.'s for
Metal–Oxygen–Carbon Bonds in $\text{Er}_2\text{Ti}_4\text{O}_2(\text{OEt})_{18}(\text{HOEt})_2$

$M-\mu_3\text{-O}$	Angle (deg)	$M-\mu\text{-O}$	Angle (deg)	$M\text{-O}_{\text{terminal}}$	Angle (deg)
Er–O1–C1A	129.5(0)	Er–O3–C3A	124.9(9)	Er–O8–C8A	169.2(15)
Ti1–O1–C1A	126.0(0)	Er–O4–C4A	123.6(10)	Er–O9–C9A	130.2(16)
Ti2–O1–C1A	24.4(0)	Er–O6–C6A	138.2(10)	Ti1–O7–C7A	129.5(15)
		Ti1–O3–C3A	124.8(11)	Ti1–O11–C11A	165.8(12)
		Ti2–O10–C10A	156.6(26)	Ti2–O10–C10A	156.6(26)
		Ti1–O5–C5A	131.9(15)		
		Ti2–O4–C4A	132.2(11)		
		Ti2–O5–C5A	124.0(15)		
		Ti2–O6–C6A	121.6(9)		

indicates that the products of the reaction are not affected by the heat treatment and thus they seem to be relatively stable against organic decomposition.

Another known way to obtain oxoalkoxides of less acidic metal ions, e.g., La, Ba, Sr, Ca, K, and Na, is to treat the solution with oxygen gas (22). A large excess of dry oxygen gas did not, however, yield more than a very small amount of $\text{Er}_2\text{Ti}_4\text{O}_2(\text{OEt})_{18}(\text{HOEt})_2$ (route 2A), and the solution gave an electronic spectrum that was very similar to that obtained without oxygen (see Fig. 1). It might be that the Er^{3+} ion is too acidic for the oxidation to take place, but a formation of Er–Ti ethoxides which increase the Er acidity might also hinder oxidation.

The most obvious way to prepare oxoalkoxides is addition of small amounts of water to non-oxo alkoxides. We have studied two ways of adding a stoichiometric amount of water: to the KOEt–Ti(OEt)₄ mixture before the ErCl_3 addition (route 1), and to the mixture formed after the ErCl_3 addition (route 2A). Either way the water is added, $\text{Er}_2\text{Ti}_4\text{O}_2(\text{OEt})_{18}(\text{HOEt})_2$ is obtained in rather high yields. Route 1 gives slightly higher yields and might also simulate less rigorously dried solvents and starting materials and therefore seems to be the best one. From the UV–Vis and IR studies, it seems that $\text{Er}_2\text{Ti}_4\text{O}_2(\text{OEt})_{18}(\text{HOEt})_2$ existed already before the evaporation for crystallization in the routes 1 and 2B, since their solution electronic spectra showed fine structures similar to that of the dissolved $\text{Er}_2\text{Ti}_4\text{O}_2(\text{OEt})_{18}(\text{HOEt})_2$ (Fig. 1).

Er metal and Ti(OEt)₄ in 4:1 toluene:ethanol did not react even on heating, but addition of a very small amount of HgCl_2 catalyzed the reaction so that it could occur at room temperature, although slowly. At 60°C (route 4), the reaction first yielded a purple solution with the electronic spectrum shown in Fig. 2, comprising peaks typical of Er^{3+} ions as well as a broad band assigned to the ${}^1E_g \leftarrow {}^1T_{2g}$ transition of octahedrally coordinated Ti^{3+} . Its maximum is found at 20,400 cm^{-1} , which corresponds to a ligand field comparable to that of the aqua complex, which has a max-

imum at 20,100 cm^{-1} (23). Thus, the Er metal reduces the Ti^{4+} ions in the $\text{Ti}(\text{OEt})_4$ to Ti^{3+} , while being dissolved as Er^{3+} . Evaporation of this solution yielded a dark powder mixed with a liquid. We have not been able to identify the components of this multiphase material with certainty. If the purple solution was not evaporated, it turned pale yellow, and the resulting electronic spectrum showed no sign of the Ti^{3+} absorption (see Fig. 2). The peaks attributable to Er^{3+} showed fine structures resembling both the oxoalkoxide and the non-oxo alkoxide (Fig. 2). Evaporation and crystallization of the solution yielded ca. 20–50% $\text{Er}_2\text{Ti}_4\text{O}_2(\text{OEt})_{18}(\text{HOEt})_2$. This is lower than for routes 1 and 2A, which is at least partly depending on the formation of insoluble Er compounds during the dissolution of the metal but might also stem from the formation of other Er–Ti alkoxides, such as the supposed non-oxo one.

3.2. Characterization and Properties of $\text{Er}_2\text{Ti}_4\text{O}_2(\text{OEt})_{18}(\text{HOEt})_2$

FT-IR Studies. An IR spectrum of crystalline $\text{Er}_2\text{Ti}_4\text{O}_2(\text{OEt})_{18}(\text{HOEt})_2$ in the range 1250–400 cm^{-1} is shown in Fig. 3. Peaks in the diagnostic region, 1200–400 cm^{-1} , were found at 1158, 1145, 1097, 1055, 925, 898, 804, 602, 561, 512, 483, 467, and 420 cm^{-1} . The band with maxima at 1158 and 1145 cm^{-1} is tentatively assigned to vibrations in the ethyl groups, those with maxima at 1097, 1055, 925, and 898 cm^{-1} are tentatively ascribed to C–O and C–C vibrations (24, 25), and that below 750 cm^{-1} is assigned to M–O stretchings. The OH stretch band of the ethanol adducts showed a maximum at 3115 cm^{-1} and shoulders at ca. 3160 and ca. 3220 cm^{-1} , indicating a relatively weak hydrogen bond.

The great similarity of the IR spectra of the crystals and 4:1 toluene:ethanol or hexane solutions indicates that the molecular structure is, to a large extent, retained when the compound is dissolved (see Fig. 3). Most peaks of the dissolved compound are found within 1 cm^{-1} from those of the solid compound, and the biggest difference found was 5 cm^{-1} , in the peak at 561 cm^{-1} . In the hexane solution spectrum, the OH stretch band has a maximum at 3112 cm^{-1} , which is very close to the value of the solid compound, indicating that the hydrogen bond also remains almost intact on dissolution in hexane.

Solubility. $\text{Er}_2\text{Ti}_4\text{O}_2(\text{OEt})_{18}(\text{HOEt})_2$ is rather soluble in toluene (0.11 M), moderately soluble in hexane (0.071 M) and 4:1 (Vol:Vol) toluene:ethanol (0.055 M) solvents, and virtually insoluble in ethanol. The compound is stable both in the solid state and in solution in the presence of a small amount of ethanol.

Behavior on Heating. Inspection of crystals in melt-sealed glass capillaries showed a melting point at 102–106°C. At the same time, a noncolored liquid, believed to be

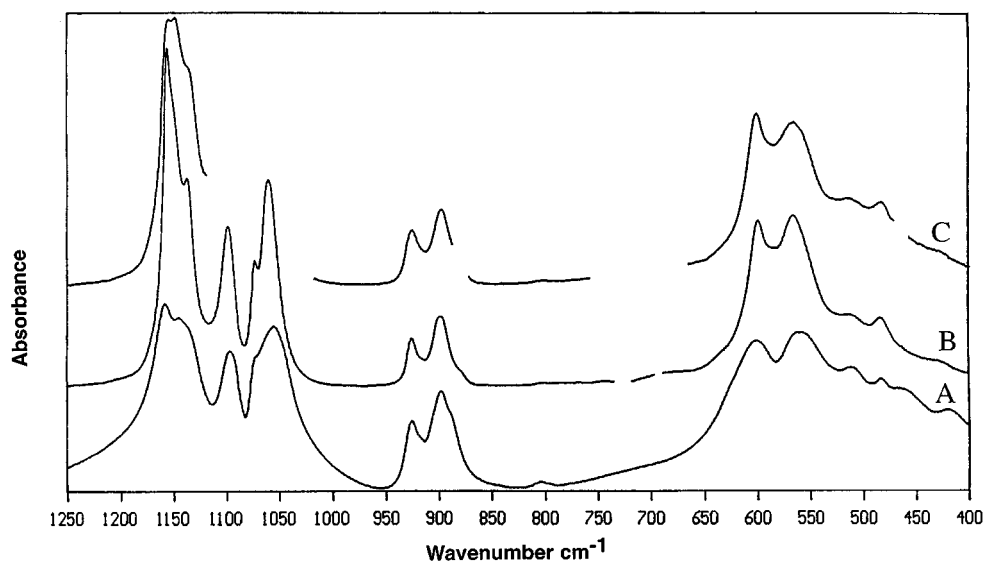


FIG. 3. FT-IR spectra of $\text{Er}_2\text{Ti}_4\text{O}_2(\text{OEt})_{18}(\text{HOEt})_2$ as a solid (A), as a hexane solution (B), and as a 0.05 M 4:1 toluene:ethanol solution (C). The plot has been removed in places where the solvent absorptions are too strong to obtain a reliable spectrum.

ethanol, was condensed in the cold end of the capillary. The resulting turbid pink melt turned clear at 201–206°C and boiled at 255–265°C, leaving a solid pink material. The DSC curve of $\text{Er}_2\text{Ti}_4\text{O}_2(\text{OEt})_{18}(\text{HOEt})_2$ is shown in Fig. 4. An endothermic peak with an onset at 101°C and a minimum at 106°C is observed in the curve. The enthalpy of this peak is ca. 220 kJ/mol, which is higher than normal for the melting of an alkoxide. It seems probable that the main part of the heat taken up from the surrounding is due to loss of the ethanol adducts, although melting was also observed visually. At higher temperatures a small endothermic peak is observed at 190–202°C, which is the temperature where the solution becomes clear. One explanation for this peak might

be that the heterobimetallic alkoxide is decomposed into one liquid and one solid alkoxide at 101–106°C and that the latter is dissolved at ca. 200°C. Further heating resulted in a boiling at 255–265°C, leaving a pink solid. This might be due to evaporation of $\text{Ti}(\text{OEt})_4$, but also to decomposition, yielding organic products.

Heating only to 120°C, followed by cooling to room temperature and a second heating, did not cause any melting or endothermic peak at 100–120°C (see Fig. 4), indicating that the loss of ethanol is nonreversible, possibly depending on a decomposition of the heterobimetallic alkoxide into two phases at 101–106°C. The behavior at higher temperatures was the same as already described, however.

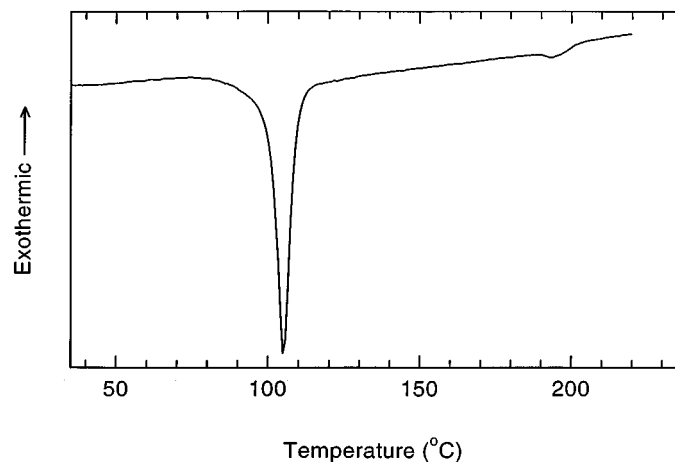


FIG. 4. A DSC curve of $\text{Er}_2\text{Ti}_4\text{O}_2(\text{OEt})_{18}(\text{HOEt})_2$ obtained in the temperature range 50–225°C.

3.3. The Structure of $\text{Er}_2\text{Ti}_4\text{O}_2(\text{OEt})_{18}(\text{HOEt})_2$

The packing sequence of the molecules can be considered as dense and body centered. The obtained molecular geometry is shown in Fig. 5, together with the atomic labeling used for the metal and oxygen atoms. Due to the restrictions imposed by the space group symmetry, the molecule is centrosymmetric, and accordingly only the labeled atoms in Fig. 5 are discussed in this paper. The center of symmetry is located at the midpoint of the rhombus formed by the two Er and the two oxo-oxygen atoms.

The bond distance distribution and calculated bond valence sums (bvs values) (26) indicate that the titanium atoms are tetravalent and the erbium atoms trivalent. Each molecule consists of two erbium, four titanium, and two oxo-oxygen atoms and twenty ethoxo groups, of which two must be protonated to achieve electroneutrality. This gives the

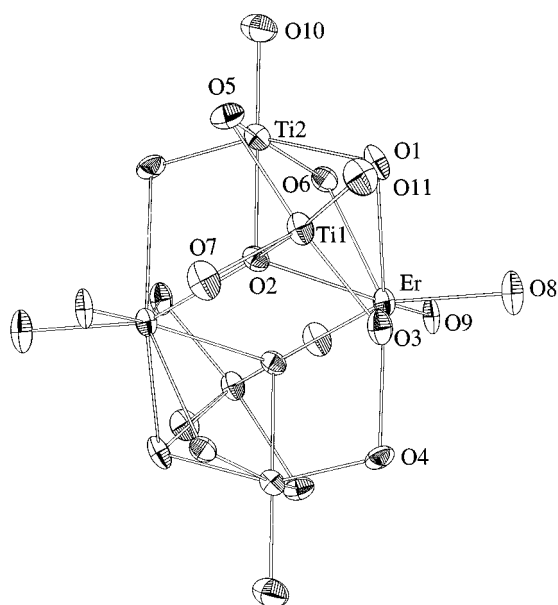


FIG. 5. Molecular structure of $\text{Er}_2\text{Ti}_4\text{O}_2(\text{OEt})_{18}(\text{HOEt})_2$. Only the metal and oxygen atoms are shown for clarity. As the molecule is centrosymmetric, only half of the atoms are labeled.

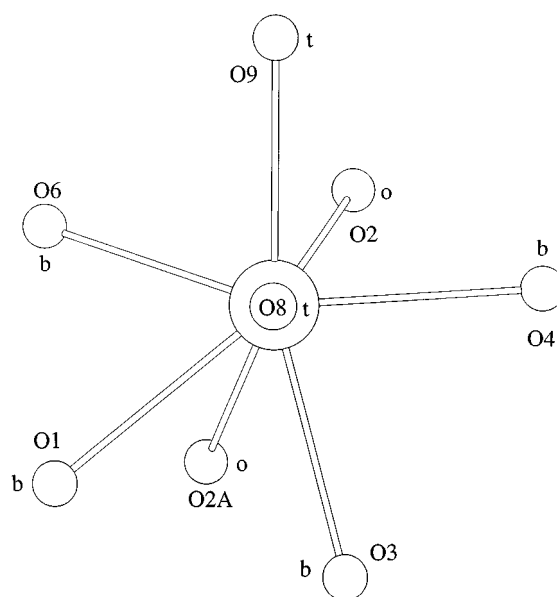


FIG. 6. Coordination figure around the Er atom seen along the Er–O8 bond. The oxygen atoms are numbered according to the labeling used in Fig. 5 and are marked b = bridging, t = terminal, and o = oxo.

molecular formula $\text{Er}_2\text{Ti}_4\text{O}_2(\text{OEt})_{18}(\text{HOEt})_2$. Taking the coordination around the oxygen atoms into account, the molecular formula becomes $\text{Er}_2\text{Ti}_4(\mu_4\text{-O})_2(\mu_3\text{-OEt})_2(\mu\text{-OEt})_8(\text{OEt})_8(\text{HOEt})_2$.

The erbium atom is eight-coordinated by five ethoxo groups, one ethanol group and two oxo-oxygen atoms. The coordination figure might be considered as a (distorted) dodecahedron, see Fig. 6. The titanium atoms are six-coordinated by five ethoxo groups and one oxo-oxygen atom. The two Ti–O octahedra share one common face, giving a slightly irregular octahedral configuration for each titanium atom.

For metal alkoxides, there are commonly occurring structure fragments of special stability, and in this molecule no less than three of the most common fragments are observed. The first one is that formed by two Er, two Ti(2), two oxo-oxygen, and four ethoxo-oxygen atoms (see Fig. 7A), also known as the C_{2h} fragment. It is known from a wide range of homometallic alkoxides, such as $\text{Ti}_4(\text{OMe})_{16}$ (12), $\text{Ti}_4(\text{OEt})_{16}$ (13), $\text{W}_4(\text{OEt})_{16}$ (27), and $\text{U}_4\text{O}_6(\text{OPh})_{10}(\text{THF})_4$ (28), as well as heterometallic ones, such as $\text{Mg}_2\text{Sb}_4(\text{OEt})_{16}$ (29), $\text{M}_2\text{Sb}_4(\text{OEt})_{16}$ ($M = \text{Ni}$ or Mn) (30), $\text{Na}_2\text{W}_2\text{O}_2(\text{OEt})_{10}(\text{HOEt})_4$ (31), $\text{Li}_2\text{Ti}_2(\text{OPr}^i)_{10}$ (14), and $\text{Li}_2\text{Nb}_2\text{O}_2(\text{OEt})_{10}(\text{HOEt})_2$ (32). The second structure fragment is the $\text{M}_2\text{M}'_2\text{O}$ configuration (see Fig. 7B), known from alkoxides such as $\text{Ce}_4\text{O}(\text{OPr}^i)_{13}(\text{HOPr}^i)$ (33), $\text{Al}_{10}\text{O}_4(\text{OEt})_{22}$ (34), $\text{Al}_4\text{O}(\text{OBu}^i)_{10}(\text{HOBu}^i)$ (35), $[\text{Sr}_2\text{Sb}_4\text{O}(\text{OEt})_{14}]_n$ (37), and $[\text{Ba}_4\text{Sb}_8\text{O}_2(\text{OEt})_{28}(\text{HOEt})]_n$ (38). The third fragment seen is the two face-sharing Ti–O octahedra, marked out in

Fig. 7C. This is also a pattern well known from e.g. $\text{BiTi}_2\text{O}(\text{OPr}^i)_9$ (10), $\text{Ba}_2\text{Zr}_4(\text{OPr}^i)_{20}$ (16), $\text{Cu}_4\text{Zr}_4\text{O}_3(\text{OPr}^i)_{18}$ (36), $\text{Ce}_2\text{Na}(\text{OBu}^i)_9$ (17), $\text{U}_2\text{K}(\text{OBu}^i)_9$ (18), $\text{BaTi}_4(\text{OEt})_{18}$ (5), $\text{Ba}_4\text{Ti}_{13}\text{O}_{18}(\text{OC}_2\text{H}_4\text{OMe})_{24}$ (9) and $\text{Cd}_2\text{Ba}_2\text{Zr}_4(\text{OPr}^i)_{24}$ (39).

Bond valence sum calculations (26) for the oxygen atoms revealed a strikingly low bvs value (1.1) for the atom labeled O9, which indicates that it is the ethanol oxygen of the molecule. The most probable proton acceptor for creating an intramolecular hydrogen bond would be an oxygen atom on another metal atom (i.e., on one of the titanium atoms), preferably on a terminal ethoxo group, for charge and sterical reasons. This gives only two alternatives, viz., O7 and O10. The interatomic distance should be rather short, which leaves only the O7 atom, with a distance of 2.637(12) Å from O9. Thus, the hydrogen bond is rather weak, which is corroborated by the relatively high wavenumber (3115 cm^{-1}) of the O–H stretch band maximum in the IR spectrum.

The erbium to oxygen bond lengths are rather consistent, with an average of 2.425 Å, but with one obvious exception, the Er–O8 distance (2.053(11) Å). Of the two terminal ethoxo oxygens, O8 and O9, the latter is involved in the hydrogen bond and therefore forms a distinctly longer bond to Er (2.38 Å).

The Ti1–O and Ti2–O bond lengths reveal that the two Ti–O octahedra are rather distorted, which is not surprising as they are face-sharing. The bond angles O1–Ti–O2, O1–Ti–O5, and O2–Ti–O5 are all quite small (average

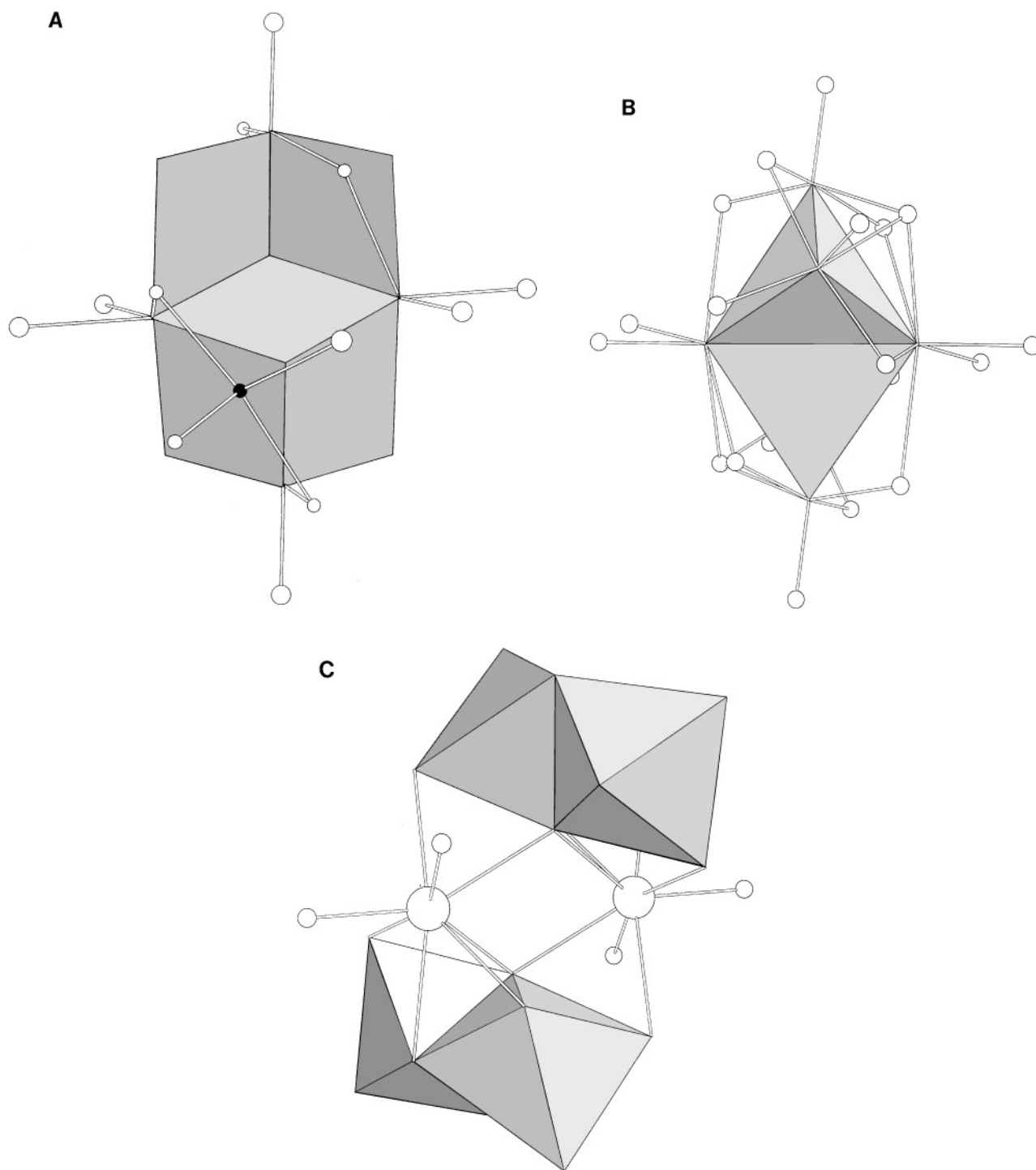


FIG. 7. The structure fragments marked out in shading: C_{2h} (A), M_2M_2O (B), and face-sharing Ti octahedra (C).

values 71.2, 76.0, and 77.2°, respectively), probably to allow a long enough distance between the Ti atoms. This distance is 3.10 Å, only 0.2 Å longer than for metallic Ti. In both coordination octahedra, the shortest Ti–O distances are found to the terminal ethoxo groups, i.e., Ti1–O7, Ti1–O11,

and Ti2–O10, with bond lengths of 1.877(11), 1.794(12), and 1.744(14) Å, respectively. The slightly longer distance between Ti1 and O7 can be explained by the fact that O7 is involved in the hydrogen bond. The Ti–O distances for bridging oxygen atoms are, with the exception of Ti–O1,

which is longer (2.14 Å), fairly equal to the average bond length (1.96 Å). For both Er–O and Ti–O bonds, the trend, in each case, of the bond lengths is in the order $\text{O}_{\text{terminal}} < \text{O}(\text{H})_{\text{terminal}} \approx \mu\text{-O} \approx \mu_4\text{-O}_{\text{oxo}} < \mu_3\text{-O}$.

The M–O–C bond angles fall roughly into two categories, one with bridging ethoxo groups and one with terminal ethoxo groups. For the bridging groups the average bond angle is 127.4° . The terminal ethoxo groups have an average bond angle of 163.9° , except for the ethanol groups, which have a much lower bond angle, 129.8° . The trends discussed above for the M–O bonds and the M–O–C angles apply also to the structures of, e.g., $M_2\text{Sb}_4(\text{OEt})_{16}$, with $M = \text{Ni}$ and Mn (15), $\text{Nd}_5\text{O}(\text{OPr}^i)_{13}(\text{HOPr}^i)_2$ (40), $\text{LaNb}_2(\text{OPr}^i)_{13}$ (41), $\text{Er}_5\text{O}(\text{OPr}^i)_{13}$ (42), and $\text{Nd}_5\text{O}(\text{OPr}^i)_{13}$ (43).

As expected, the thermal vibration amplitudes increase along the ethoxo groups toward their methyl ends. The relatively weak van der Waals forces will allow the ethoxo groups to have relatively large thermal vibrations, and therefore lower the relevance of the positions of the ethoxo groups, especially the methyl groups, obtained by single-crystal X-ray diffraction. Auxiliary material is available.¹

4. CONCLUDING REMARKS

The reaction between KOEt, $\text{Ti}(\text{OEt})_4$, and ErCl_3 , in the ratio 3:2:1, probably yields alkoxide(s) without oxo-oxygen atoms, but these could not be isolated by crystallization. Addition of stoichiometric amounts of water to the reaction mixture produced the solid and isolable oxoalkoxide $\text{Er}_2\text{Ti}_4\text{O}_2(\text{OEt})_{18}(\text{HOEt})_2$ in high yields. Treatment with oxygen gas or heating of the alkoxide mixture did not cause oxidation or decomposition to the isolable oxoalkoxide. The dissolution of Er metal together with $\text{Ti}(\text{OEt})_4$ in the ratio 1:2 produced $\text{Er}_2\text{Ti}_4\text{O}_2(\text{OEt})_{18}(\text{HOEt})_2$ via intermediates containing Ti^{3+} , although in lower yields than the hydrolysis.

The structure has been determined by single-crystal X-ray diffraction techniques. The molecule contains three of the most common structure fragments known for metal alkoxides, viz. C_{2h} , $M_2M'_2\text{O}$, and face-sharing octahedra. FT-IR studies show that the structure is retained to a large extent in 4:1 toluene:ethanol or hexane solution. Heating caused a loss of the ethanol adducts and melting at 101°C .

The alkoxide molecule contains two adjacent Er atoms and is, therefore, not a suitable precursor for our studies on

preparation of Er-doped waveguides, using alkoxides containing single, isolated Er atoms. The alkoxide should, however, be a good precursor in ordinary sol–gel processing of various oxide materials for optics, sensors, oxygen conductors, and construction ceramics.

ACKNOWLEDGMENTS

Dr. K. Jansson is thanked for performing the DSC measurements. This research was supported by the Swedish National Science Research Council. M. W. thanks the Royal Science Academy for financial support.

REFERENCES

1. K. G. Caulton and L. G. Hubert-Pfalzgraf, *Chem. Rev.* **90**, 969 (1990).
2. C. D. Chandler, C. Roger, and M. J. Hampden-Smith, *Chem. Rev.* **93**, 1205 (1993).
3. M. Wijk, R. Norrestam, M. Nygren, and G. Westin, *Inorg. Chem.* **35**, 1077 (1996).
4. V. W. Day, T. A. Eberspacher, W. G. Klemperer, C. W. Park, and F. S. Rosenberg, *J. Am. Chem. Soc.* **113**, 8190 (1991).
5. M. I. Yanovskaya, E. P. Turevskaya, V. G. Kessler, I. E. Obvintseva, and N. Ya. Turova, *Integr. Ferroelectr.* **1**, 343 (1992).
6. K. Watenpaugh and C. N. Caughlan, *Chem. Commun.* **2**, 76 (1967).
7. R. Schmid, A. Mosset, and J. Galy, *J. Chem. Soc., Dalton Trans.* 1999 (1991).
8. A. I. Yanovsky, M. I. Yanovskaya, V. K. Limar, V. G. Kessler, N. Ya. Turova, and Y. T. Struchkov, *J. Chem. Soc., Chem. Commun.* 1605 (1991).
9. J.-F. Campion, D. A. Payne, H. K. Chae, J. K. Maurin, and S. R. Wilson, *Inorg. Chem.* **30**, 3245 (1991).
10. R. Papiernik, L. G. Hubert-Pfalzgraf, S. Parola, S. Jagner, F. Soares-Carvalho, P. Thomas, and J. P. Mercurio, "Better Ceramics through Chemistry VI" (A. J. Cheetham, C. J. Brinker, M. L. Mecartney, and C. Sanchez, Eds.), p. 285. Materials Research Society, Pittsburgh, PA, 1994. [Meter. Res. Soc. Proc. Vol. 364]
11. S. Daniele, L. G. Hubert-Pfalzgraf, J.-C. Daran, and S. Halut, *Polyhedron* **13**, 927 (1994).
12. D. A. Wright and D. A. Williams, *Acta Crystallogr., B* **24**, 1107 (1968).
13. J. A. Ibers, *Nature* **197**, 686 (1963).
14. M. J. Hampden-Smith, D. S. Williams, and A. L. Reingold, *Inorg. Chem.* **29**, 4076 (1990).
15. E. P. Turevskaya, V. G. Kessler, N. Ya. Turova, A. P. Pisarevsky, A. I. Yanovsky, and Y. T. Struchkov, *J. Chem. Soc., Chem. Commun.* 2303 (1994).
16. B. A. Vaartstra, J. H. Huffman, W. E. Streib and K. G. Caulton, *J. Chem. Soc., Chem. Commun.* 1750 (1990).
17. W. J. Evans, T. J. Deming, J. M. Olofson, and J. W. Ziller, *Inorg. Chem.* **28**, 4027 (1989).
18. F. A. Cotton, D. O. Marler, and W. Schwotzer, *Inorg. Chem.* **23**, 4211 (1984).
19. "International Tables for X-Ray Crystallography," Vol. IV. Kynoch, Birmingham, 1974.
20. SHELXTL PC™, release 4.1, Siemens Analytical X-ray Instruments Inc., 1990.
21. K. B. Yatsimirskii and N. K. Davidenko, *Coord. Chem. Rev.* **27**, 223 (1979).
22. N. Ya. Turova, E. P. Turevskaya, V. G. Kessler, A. I. Yanovsky, and Y. T. Struchkov, *J. Chem. Soc., Chem. Commun.* 21 (1993).
23. A. B. P. Lever, "Inorganic Electronic Spectroscopy," 2nd ed. Elsevier, Amsterdam, 1984.

¹ See NAPS document No. 05433 for 21 pages of supplementary material. This is a multi-article document. Order from NAPS c/o microfiche Publications, P.O. Box 3513, Grand Central Station, New York, NY 10163-3513. Remit in advance U.S. funds only \$7.75 for photocopies or \$5.00 for microfiche. There is a \$15.00 invoicing charge on all orders filled before payment. Outside U.S. and Canada add postage of \$4.50 for the first 20 pages and \$1.00 for each 10 pages of material thereafter, or \$1.75 for the first microfiche and \$.50 for each microfiche thereafter.

24. C. G. Barraclough, D. C. Bradley, J. Lewis, and I. M. Thomas, *J. Chem. Soc.* 2601 (1961).
25. D. C. Bradley, R. C. Mehrotra, and D. P. Gaur, "Metal Alkoxides." Academic Press, London, 1978.
26. I. D. Brown and D. Altermatt, *Acta Crystallogr., B* **41**, 244 (1985).
27. M. H. Chisholm, J. C. Huffman, C. C. Kirkpatrick, J. Leonelli, and K. Folting, *J. Am. Chem. Soc.* **103**, 6093 (1981)
28. W. G. van der Sluys and A. P. Sattelberger, *Chem. Rev.* **90**, 1027 (1990).
29. U. Bemm, K. Lashgari, R. Norrestam, M. Nygren, and G. Westin, *J. Solid State Chem.* **103**, 366 (1993).
30. U. Bemm, R. Norrestam, M. Nygren, and G. Westin, *Acta Crystallogr., C* **51**, 1260 (1995).
31. N. Ya. Turova, V. G. Kessler, and S. I. Kucheiko, *Polyhedron* **10**, 2617 (1991).
32. A. I. Yanovskii, E. P. Turevskaya, N. Ya. Turova, and Yu. T. Struchkov, *Sov. J. Coord. Chem.* **11**, 110 (1985).
33. K. Yunlu, P.S. Gradeff, N. Edelstein, W. Kot, G. Shalimoff, W. E. Streib, B. A. Vaartstra, and K. G. Caulton, *Inorg. Chem.* **30**, 2317 (1991).
34. A. I. Yanovskii, N. Ya. Turova, N. I. Kozlova, and Yu. T. Struchkov, *Sov. J. Coord. Chem.* **13**, 149 (1987).
35. R. A. Sinclair, M. L. Brostrom, W. B. Gleason, and R. A. Newmark, "Better Ceramics through Chemistry V" (M. J. Hampden-Smith, W. G. Klemperer and C. J. Brinker, Eds.), p. 27. Materials Research Society, Pittsburgh, PA, 1992. (Mater. Res. Soc. Symp. Proc. Vol. 271).
36. J. A. Samulels, B. A. Vaartstra, J. C. Huffman, K. L. Trojan, W. E. Hatfield, and K. G. Caulton, *J. Am. Chem. Soc.* **112**, 9623 (1990).
37. U. Bemm, R. Norrestam, M. Nygren, and G. Westin, *J. Solid State Chem.* **108**, 243 (1994).
38. U. Bemm, K. Lashgari, R. Norrestam, M. Nygren, and G. Westin, in press.
39. M. Veith, S. Mathur, and V. Huch, *J. Am. Chem. Soc.* **118**, 903 (1996).
40. G. Helgesson, S. Jagner, O. Poncelet, and L. G. Hubert-Pfalzgraf, *Polyhedron* **10**, 1559 (1991).
41. A. I. Yanovskii, E. P. Turevskaya, N. Ya. Turova, F. M. Dolgushin, A. P. Pisarevskii, A. S. Batsanov, and Yu. T. Struchkov, *Russ. J. Inorg. Chem.* **39**, 1246 (1994).
42. M. Wijk, M. Kritikos, and G. Westin. [in preparation]
43. M. Kritikos, M. Wijk, and G. Westin. [in preparation]